

Research Article

Investigation of highly efficient CO₂ hydrogenation at ambient conditions using dielectric barrier discharge plasma

Zhihao Zeng^{a,b,c,1}, Yujiao Li^{a,b,1}, Yunfei Ma^a, Xiaoqing Lin^a, Xiangbo Zou^c, Hao Zhang^a, Xiaodong Li^a, Qingyang Lin^a, Ming-Liang Qu^d, Zengyi Ma^{a,b,**}, Angjian Wu^{a,b,*}

^a State Key Laboratory of Clean Energy Utilization, Zhejiang University, Hangzhou, 310027, China

^b Ningbo Innovation Center, Zhejiang University, China

^c LTD. Cosin Solar Technology Co., Ltd, China

^d Department of Earth Science and Engineering, Imperial College London, SW7 2AZ, UK

ARTICLE INFO

Keywords words:

CO₂ hydrogenation
Dielectric barrier discharge (DBD) plasma
Nonthermal equilibrium
CO₂ utilization
Ambient conditions

ABSTRACT

The increasing utilization of CO₂ for synthesizing high-value fuels or essential chemicals is a potentially effective approach to mitigating global warming and climate change. Compared to thermal catalytic CO₂ conversion under harsh operating conditions (400~500°C, 10 MPa), non-thermal plasma can overcome kinetic barriers and trigger reactions beyond thermal equilibrium at ambient temperature and pressure. In this study, the effects of operating conditions (discharge frequency, input power, and gas flow rate) and geometrical parameters (discharge length, discharge gap, and dielectric materials) have been extensively analyzed using typical cylindrical dielectric barrier discharge (DBD) plasma. The discharge characteristics changed by operating conditions (including waveforms of applied voltage and current) are compared, indicating higher applied voltage and lower gas flow rate can strengthen the filamentary discharges. The results demonstrate CO₂ conversion rate increases with the increase of applied voltage and the decrease of CO₂/H₂ ratio, achieving its maximum value of 43.0% at 20 mL/min. The highest energy efficiency of 3771.9 μg/kJ for CO generation is obtained at the applied voltage of 5.5 kV and gas flow rate of 40 mL/min, respectively. Besides, the structure of plasma reactor also impacts the performance of CO₂ conversion. On the one hand, the discharge gap has a significant role in the variation of CO₂ conversion and product selectivity, which is attributed to the electric field density and corresponding electron-induced reaction. On the other hand, the circulating water-cooling jacket was used to find out the influence of reaction temperature, which switched the product from CO to CH₄. This work will pave the way for a sustainable alternative towards future CO₂ conversion and utilization.

1. Introduction

The rapid rise of CO₂ emissions has attracted global attention due to its long-term impact on climate change and ocean acidification (Kanuri et al., 2024). According to statistics, global carbon dioxide emissions approached nearly 41.3 gigatons with an average per capita emission of 5.2 tons in 2022 (<https://www.iea.org/reports/ccus-in-clean-energy-transitions>) (IEA, 2020). Effective conversion of CO₂ into versatile carbon-based fuels or chemicals (e.g., CO, methanol, ethylene, etc.) via advanced catalytic hydrogenation processes has been recognized as a promising route to alleviate global warming while recycling and

upgrading the utilization of captured massive CO₂ from industrial emissions (Shin et al., 2021; Wei et al., 2021; Zhai et al., 2020). Nevertheless, the stubborn CO bond of CO₂ (805 kJ/mol) is hard to activate and further convert under mild conditions (Zhang et al., 2023). For traditional thermal-catalytic CO₂ hydrogenation, stringent operating conditions such as high temperature and pressure (400~500°C, 10 MPa) are required to maintain reaction activity (Kondratenko et al., 2013; Modak et al., 2020). Even though the single-step conversion rate (<20%) and total reaction efficiency are still relatively low (Álvarez et al., 2017; Karakaya and Parks, 2023; Olah et al., 2009; Tada et al., 2021), resulting in high energy consumption for large-scale industrial applications

* Corresponding author. State Key Laboratory of Clean Energy Utilization, Zhejiang University, Hangzhou, 310027, China.

** Corresponding author. State Key Laboratory of Clean Energy Utilization, Zhejiang University, Hangzhou, 310027, China.

E-mail addresses: mazy@zju.edu.cn (Z. Ma), wuaj@zju.edu.cn (A. Wu).

¹ The authors contributed equally.

(Schwiderowski et al., 2022). There were no obvious mistakes in the text. I made some minor adjustments for better readability.

Non-thermal plasma has emerged as an effective technology to activate CO₂ at ambient conditions (Wanten et al., 2023). Distinct from conventional thermal catalysis, the energy injected into plasma is selectively transferred into active species via different reaction channels (such as electronic excitation, ionization, and dissociation, etc.) (Chaudhary et al., 2020; Zeng and Tu, 2017), rather than converted into heat dissipating into the surrounding environment. Thus, the gas temperature can remain at room temperature while the temperatures of electron energy and excited molecules range from 1 to 10 eV and 0.1~2 eV, respectively (Chen et al., 2020). Attributed to these highly active species (energetic electrons, atoms, ions, vibrational/rotational activated molecules), non-thermal plasma can overcome kinetic barriers and trigger reactions beyond thermal equilibrium at ambient temperature and pressure (Chen et al., 2024). Among various non-thermal plasma technologies (corona discharge, microwave discharge, gliding arc discharge, etc.), dielectric barrier discharge (DBD) plasma, with the merits of flexible reactor configuration, low energy consumption, and compatibility with heterogeneous catalysis, has attracted widespread attention for various applications, including volatile organic compounds (VOCs) decomposition, surface treatment, and ozone generation (Ullah et al., 2023).

Recently, emerging research has been conducted on CO₂ conversion using DBD plasma to synthesize CO, methanol, and CH₄. (Li et al., 2023; Ray et al., 2021; Wu et al., 2023). The effects of operating conditions (discharge frequency, input power, and gas flow rate) and geometrical parameters (discharge length, discharge gap, and dielectric materials) have been extensively analyzed. Additionally, numerical modeling has also been conducted to gain in-depth insights into the chemical behavior of DBD plasma in CO₂ conversion (Huang et al., 2023). For instance, Aerts et al. (2015) utilized DBD plasma for CO₂ decomposition, demonstrating the discharge gap affected the micro-discharge, while the discharge frequency exhibited a negligible effect on gas conversion rate and energy efficiency. However, Ozkan et al. (2017) pointed out that both CO₂ conversion rate and energy efficiency significantly decreased with the increase of discharge frequency from 15 to 30 kHz. It was suggested the optimal discharge frequency depended on the input power and could not directly correlate the discharge frequencies to CO₂ conversion rate and energy efficiency (Paulussen et al., 2010). Duan et al. (2015) investigated the influence of filled dielectric material, including particle size, dielectric constant, surface acidity, and alkalinity, on CO₂ conversion and energy efficiency (Duan et al., 2015). However, systematic consideration of DBD plasma-driven CO₂ hydrogenation combined with experiments and advanced characterization is inadequate, which is significant for further upgrading product value or integrating with other processes.

Herein, we employ a cylindrical DBD plasma reactor to investigate the influence of operating parameters and configuration on the performance of CO₂ conversion. Firstly, V-I characteristics, including waveforms of applied voltage and current, are recorded and analyzed by the oscilloscope. Through single-variable experiments, the impact of operating conditions such as applied voltage, CO₂/H₂ ratio, and gas flow rate is systematically investigated, in terms of the product selectivity, yield, energy efficiency, and CO₂ conversion rates. On the other hand, the effect of reactor structure and discharge gap is also compared with a circulating water-cooling reactor. Compared with the traditional reactor, gas production distribution varies from CO to CH₄, reaching the maximum CH₄ selectivity of 18.9%. This work will lay a solid foundation for a sustainable alternative in future CO₂ conversion and utilization.

2. Experimental setup and methods

2.1. Coaxial cylindrical DBD plasma reactor

The low-temperature plasma reactor is a coaxial cylindrical dielectric barrier discharge reactor. The reactor consists of inlet and outlet

pipelines at the upper and lower ends, which are used for the input of raw gas and output of gaseous products. A high-temperature-resistant tungsten steel rod is centrally placed in the reactor as the inner electrode, connecting to the high-voltage electrode of the AC plasma power source. The outer surface of the quartz tube is wrapped with stainless steel wire mesh serving as an external ground electrode. The outer diameter of the reactor quartz tube is 12 mm, with a quartz dielectric layer thickness of 2 mm. The discharge gap is flexibly tunable, ranging from 1 to 3 mm while the total effective discharge length remains at 50 mm.

2.2. Experimental methods and apparatus

The scheme of hydrogenation experimental equipment is shown in Fig. 1. The flow rates of CO₂ and H₂ were controlled by a mass flow controller (Seven Star CS200A) and calibrated by a soap film flowmeter, ranging from 20 to 100 mL/min. Different CO₂/H₂ ratios were supplied by setting the individual gas flows to change from 1:3 to 3:1. The gas chromatograph (GC, FULI 9790 II) was equipped with a thermal conductivity detector (TCD) and flame ionization detector (FID) to measure the gas concentrations and had been calibrated using standard gas cylinders. The quantitative analysis was performed using an external standard method for detection. The pipelines between the DBD reactor and the gas chromatography were wrapped with insulation tapes to prevent the condensation of products. The discharge characteristics, including applied voltage and current, were controlled and detected by the plasma power supply (CTP-2000K) and the oscilloscope (Tektronix DPO4034B), respectively. The voltage amplitude was up to 10.5 kV with a fixed frequency of 27,500 Hz. Furthermore, the charge was measured by a voltage probe across a measuring capacitor (0.47 μF). To explore the influence of the DBD plasma reactor, two different ground electrode structures were compared for CO₂ hydrogenation. Herein, reactor II (water-electrode reactor) replaced the stainless steel mesh with a circulating water cooling jacket with built-in metal wire for conductivity based on reactor I (traditional cylindrical DBD plasma reactor), and NaCl was added to the circulating water to enhance conductivity.

2.3. Evaluation of CO₂ hydrogenation via DBD plasma

The P, Q, and effective capacitances are calculated by the formulas (Brandenburg et al., 2023):

$$P = \frac{1}{T} \int_0^T U I dt = f \cdot C_m \int U dU_m \quad (1)$$

$$f = \frac{1}{T} (\text{Hz}) \quad (2)$$

$$dQ = I dt = d(C_m \cdot U_m) = C_m dU_m \quad (3)$$

$$\zeta_{\text{effective}}(PF) = \frac{dQ}{dV} = C_m \frac{U_m}{U} \quad (4)$$

where P (W), U (kV), and I (A) represent power, applied voltage, and current. C_m = 0.47 × 10⁻⁶ F, f (Hz), T (s), Q (C), and U_m (V) are the frequency, time cycle, charges, and voltage across the capacitor. ζ_{effective} represents the effective capacitance during the discharge.

The CO₂ conversion rate is evaluated by the ratio of the amount of converted CO₂ material to the amount of input CO₂ material as follows:

$$X_{\text{CO}_2} = \frac{Q_{\text{in}} (\text{mol/min}) \times C_{(\text{CO}_2\text{-in})} (\%) - Q_{\text{out}} (\text{mol/min}) \times C_{(\text{CO}_2\text{-out})} (\%)}{Q_{\text{in}} (\text{mol/min}) \times C_{(\text{CO}_2\text{-in})} (\%)} \quad (5)$$

where Q_{in} and Q_{out} represent the total gas flow rate at the inlet and outlet of the reaction, while C_(CO₂•in) and C_(CO₂•out) represent the concentration of CO₂ in the inlet and outlet gases.

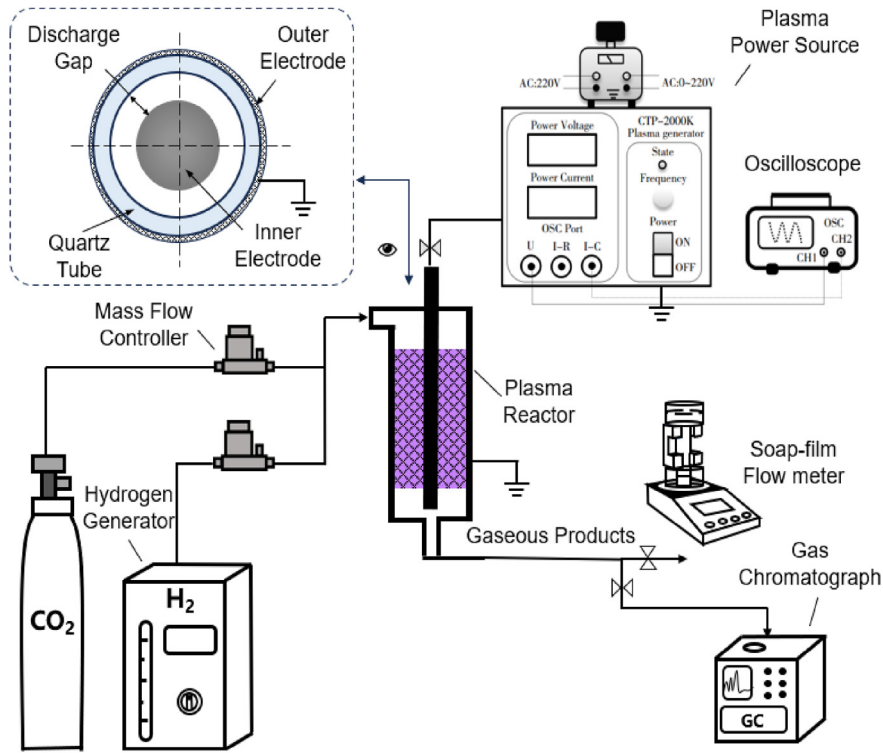


Fig. 1. The scheme of the DBD plasma-driven CO₂ hydrogenation system.

The selectivity of the product is calculated as follows:

$$S_{\text{CO}} (\%) = \frac{Q_{\text{out}} (\text{mol/min}) \times C_{\text{CO}\bullet\text{out}} (\%) }{Q_{\text{con}} (\text{mol/min})} \quad (6)$$

$$S_{\text{CH}_4} (\%) = \frac{Q_{\text{out}} (\text{mol/min}) \times C_{\text{CH}_4\bullet\text{out}} (\%) }{Q_{\text{con}} (\text{mol/min})} \quad (7)$$

Amongst, Q_{con} is the amount of converted CO₂, which equals the carbon dioxide in the feed gas minus that in the product. The carbon dioxide in the product is measured by gas chromatography. S_{CO} and S_{CH_4} represent the selectivity of CO and CH₄. The concentration of CO and CH₄ is indicated as $C_{\text{CO}\bullet\text{out}}$ and $C_{\text{CH}_4\bullet\text{out}}$, respectively.

The energy efficiency (EE) for generating CO and CH₄ is defined as the amount of CO or CH₄ produced per unit input energy (kJ).

$$EE_{\text{CO}} (\mu\text{g/kJ}) = \frac{Q_{\text{out}} (\text{mol/s}) \times C_{\text{CO}\bullet\text{out}} (\%) \times 28 (\text{g/mol}) \times 10^9 (\mu\text{g} \cdot \text{J/g} \cdot \text{kJ})}{P (\text{W})} \quad (8)$$

$$EE_{\text{CH}_4} (\mu\text{g/kJ}) = \frac{Q_{\text{out}} (\text{mol/s}) \times C_{\text{CH}_4\bullet\text{out}} (\%) \times 16 (\text{g/mol}) \times 10^9 (\mu\text{g} \cdot \text{J/g} \cdot \text{kJ})}{P (\text{W})} \quad (9)$$

The yield of CO and CH₄ is calculated by the product of the CO₂ conversion rate and product selectivity as follows:

$$Y_{\text{CO}} (\%) = X_{\text{CO}_2} \times S_{\text{CO}} (\%) \quad (10)$$

$$Y_{\text{CH}_4} (\%) = X_{\text{CO}_2} \times S_{\text{CH}_4} (\%) \quad (11)$$

The specific energy density (SEI) of a plasma reaction is calculated as follows:

$$SEI (\text{kJ/L}) = \frac{P (\text{kW})}{F (\text{L/s})} \quad (12)$$

where F represents the total volumetric flow rate of reactant gases. The products are measured by gas chromatography after the stable discharge of plasma. Therefore, we assume that the concentrations of the gaseous products remain stable during the measurement time. The absolute amount of gas products can be calculated by reaction time and flow rate.

$$V_{\text{all}} (\text{mL}) = v (\text{mL/min}) \times t (\text{min}) \quad (13)$$

$$V_{\text{CO}_2} (\text{mL}) = C_{\text{CO}_2} (\%) \times V_{\text{all}} (\text{mL}) \quad (14)$$

where V_{all} (mL), v (mL/min), and t (min) represent total gas volume, flow rate, and reaction time. The V_{CO_2} (mL) and C_{CO_2} (%) are the absolute volume and relative concentration of carbon dioxide.

3. Results and discussion

3.1. Analysis of electrical characteristics during CO₂ hydrogenation in DBD plasma

In Fig. 2(a) and (b), the waveforms of applied voltage and current are presented. More intensive micro-discharges are generated by increasing the applied voltage from 5.5 to 10.5 kV. The peak-to-peak voltage and current increase from 11 to 21 kV and from 38.6 to 128.1 mA, correspondingly. When the applied voltage is below 8.5 kV, few DBD filamentary discharges are generated, resulting in less conductive species and a lower concentration of charged particles (ions and electrons) (George et al., 2021). The applied voltage increases from 5.5 to 8.5 kV, triggering more intense electron-collision-induced reactions to activate carbon dioxide molecules and break the C=O bond, thereby strengthening the filamentary discharge and the discharge glow. However, when the applied voltage further increases from 8.5 to 10.5 kV, the number of micro-discharges does not change significantly. It is assumed that the amounts of charges deposited on the surface of the dielectric layer saturate at a certain level, thereby preventing further charge transmission. The liner fitting curve presented in Fig. 2(c) indicates that the

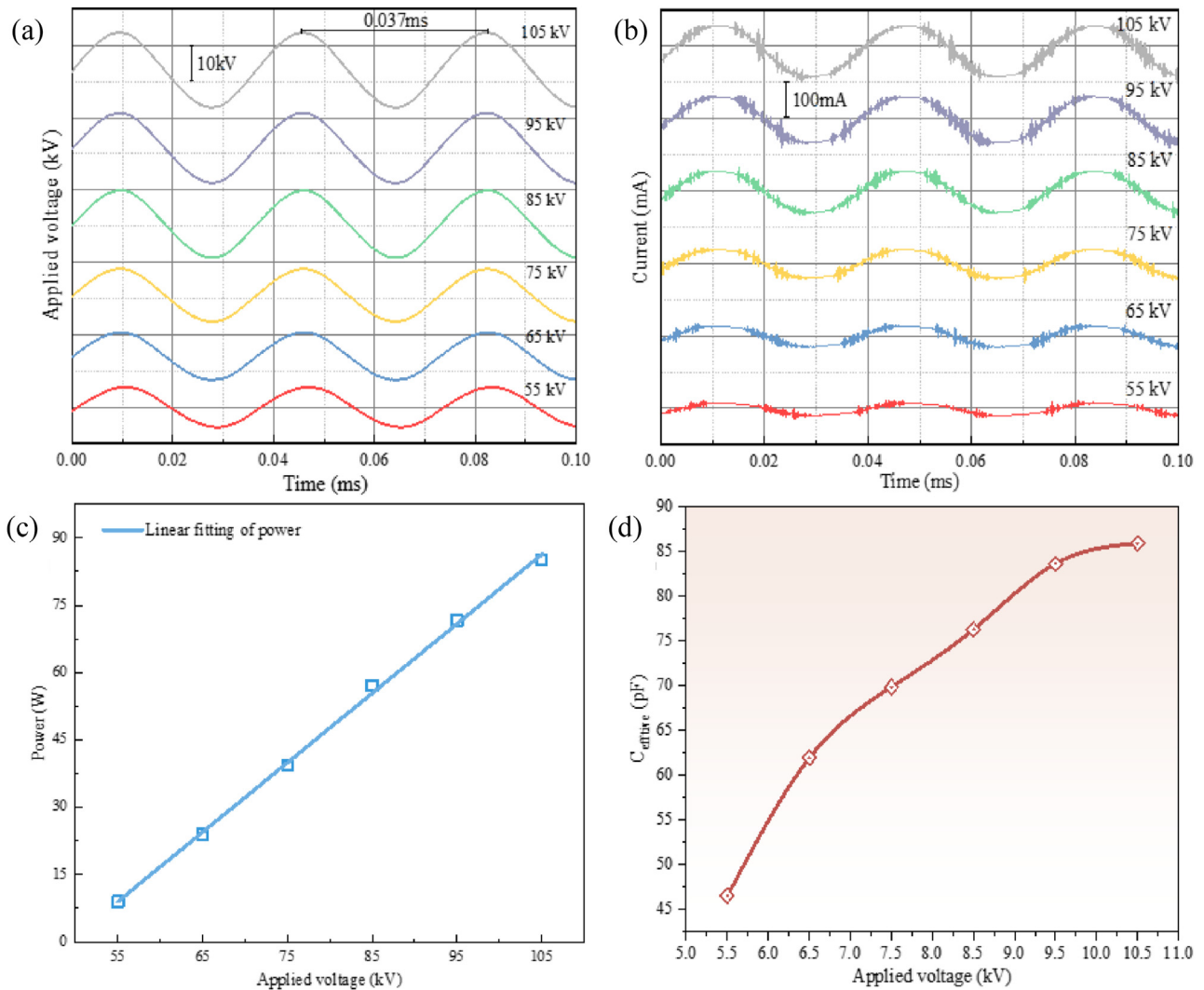


Fig. 2. Electrical parameters analysis of CO₂ hydrogenation in DBD plasma (the discharge gap is 1 mm). (a) Voltage waveforms (b) Current waveforms (c) input power dependent on the variation of applied voltage (from 5.5 kV to 10.5 kV) (d) effective capacitances during the discharge (corresponds to gas flow rate = 40 mL/min and CO₂/H₂ ratio = 1:1).

input power rises linearly with the increase of the applied voltage within the range of 5.5~10.5 kV. Since the applied voltage is easy to precisely control and increase uniformly, we draw the curve of output variation with the applied voltage as the abscissa. To explore the mechanism of the increased voltage on CO₂ conversion, the plasma coverage is calculated according to Equations 15–18. The DBD reactor can be simply equivalent to two capacitances arranged linearly, which was introduced by Peeters and van de Sanden (Peeters and Van de Sanden, 2014). C_{diel} is equal to the dielectric barrier layer, while C_{gap} presents the discharge gap, together forming the total capacitance C_{cell} . The non-uniform plasma discharge consists of many individual discharge channels, thereby forming filamentary micro-discharges. The filamentary discharges are consistent with the observation of electrical characteristics presented in Fig. 2(a) and (b). However, the micro-discharges do not occur simultaneously and do not cover the entire dielectric surface. In this case, the steepest slope, defined as the effective dielectric capacitance ξ_{diel} , will be lower than C_{diel} . The electrode area is divided into the non-discharge part (characterized by the parameter α) and the discharge part (parameter β), where $\alpha + \beta = 1$. The relationships are defined as follows (Mahdikia et al., 2023; Peeters and Van de Sanden, 2014).

$$\alpha + \beta = 1 \quad (15)$$

$$\alpha = \frac{C_{diel} - \xi_{diel}}{C_{diel} - C_{cell}} \quad (16)$$

$$\beta = \frac{\xi_{diel} - C_{cell}}{C_{diel} - C_{cell}} \quad (17)$$

$$\xi_{diel} = \alpha C_{cell} + \beta C_{diel} \quad (18)$$

The effective dielectric capacitance ξ_{diel} is used to represent the effective discharge area, that is, the plasma coverage. According to Fig. 2(d), it can be found that the effective capacitance increases from 46.6 to 85.9 pF when the applied voltage increases from 5.5 to 10.5 kV, indicating that the discharge part and plasma coverage in the reaction zone increase significantly, thereby promoting the conversion of carbon dioxide.

3.2. Influence of operating conditions on CO₂ hydrogenation in DBD plasma

3.2.1. The influence of applied voltage

As shown in Fig. 3, the conversion rate of carbon dioxide changes significantly with the increase of applied voltage at a lower applied voltage. When the applied voltage increases from 5.5 to 8.5 kV, the CO₂

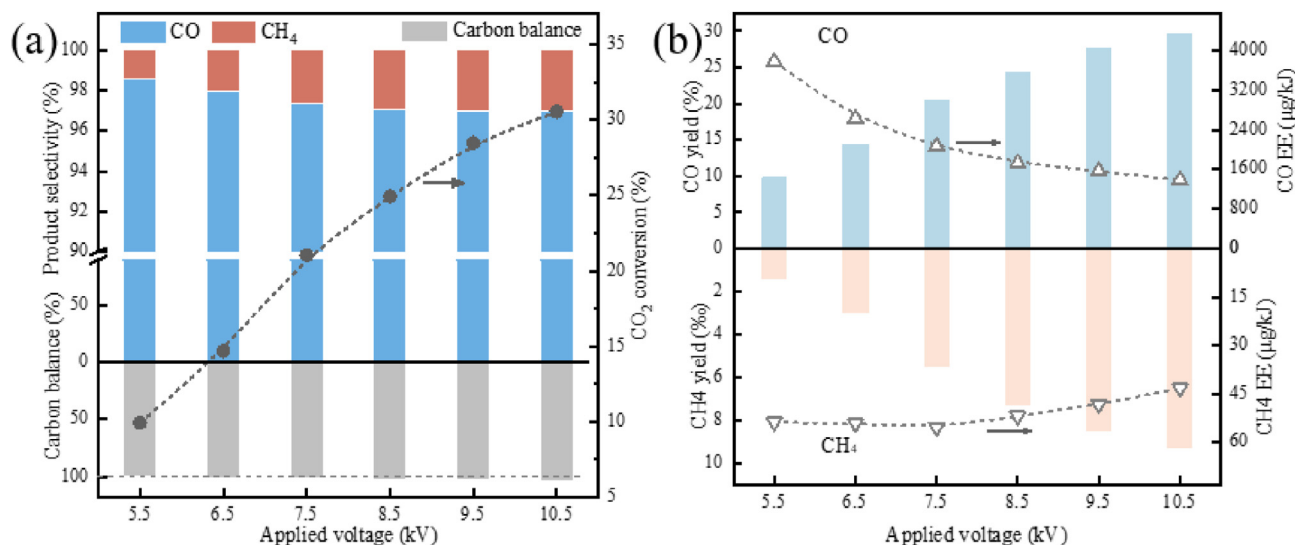
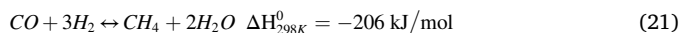
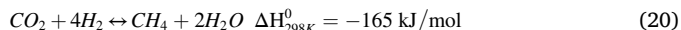
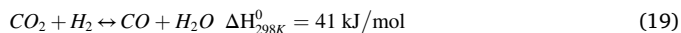


Fig. 3. The influence of applied power on (a) CO₂ conversion, product selectivity and carbon balance; (b) product yield and efficiency (CO and CH₄) (gas flow rate of 40 mL/min and CO₂/H₂ ratio of 1:1, respectively). The discharge gap is 1 mm.

conversion rate increases from 9.9% to 21.1%. The electric field intensity increases significantly with the rise in the energy input, facilitating the shift of the electron energy to a higher energy density distribution. The CO₂ conversion rate increases slightly (5.6%) by further increasing applied voltage from 8.5 to 10.5 kV, which is consistent with the tendency of electrical characteristics. As shown in Fig. 3(a), the main products are CO and CH₄. The CH₄ selectivity increases from 1.4% to 3.0% with the increase of applied power, which might be attributed to rich H atoms. Besides, the carbon balance based on mass balance is calculated before and after the reaction to avoid the potential loss caused by the liquid products. Almost 100% carbon balance is realized at each applied voltage to ensure the accuracy of CO₂ conversion and product selectivity. In Fig. 3(b), with the increase of applied voltage, the yield of CO and CH₄ increases from 9.8% to 29.6% and from 0.1% to 0.9%, respectively. In contrast, the energy efficiency of CO and CH₄ demonstrates a decreasing tendency. It is speculated that the lower applied power promotes electron-induced channels such as electronic excitation and vibrational excitation, facilitating the CO₂ activation and hydrogenation. When the applied voltage changes from 5.5 to 10.5 kV, the energy efficiency of CO decreases from 3771.9 to 1384.5 µg/kJ.

CO is probably produced by the reverse water-gas shift (RWGS) reaction.



The RWGS reaction is endothermic while the CH₄ formation is exothermic, indicating that high temperature is conducive to the forward progress of the RWGS reaction. (Eliasson et al., 1998). When the applied voltage is increased from 5.5 to 10.5 kV, more energy is dissipated into heat via channels such as vibrational-translational relaxation, leading to a rise in temperature within the center reaction area from 65 to 241°C (±2°C) recorded by an Infrared thermal imaging thermometer (FLUKE Ti32). During this process, the formation of methane is thermodynamically limited, ultimately leading to a decrease in product energy efficiency (Fig. S1). However, higher applied voltage favors methanation formation, illustrating that more active radical reactions generated by high temperatures are beneficial to methanation.

3.2.2. Influence of CO₂/H₂ ratio

Fig. 4 illustrates the impact of the CO₂/H₂ ratio on the overall performance at the fixed gas flow rate and applied power. Fig. 4(c) illustrates the applied power stays almost still when the gas distribution ratio changes from 1:3 to 3:1, which means it has little impact on energy efficiency. The increase in energy efficiency mainly comes from the change of gas distribution ratio. The CO₂ conversion rate continuously decreases with the reduction of H₂ proportion in the gas mixture. This variation tendency is similar to thermal catalytic processes. When CO₂/H₂ gas ratio changes from 1:3 to 3:1, CO₂ conversion rate drops from 28.1% to 15.0%. Concurrently, the selectivity of CH₄ also decreases from 4.3% to 0.8%. The product yield, energy efficiency, and yields of CH₄ and CO all decrease with the increase of the CO₂/H₂ ratio from 1:3 to 3:1. Interestingly, CO and CH₄ exhibit distinctly different trends in energy efficiency. The energy efficiency of CO continuously increases from 1349.8 to 2306.2 µg/kJ, while the efficiency of CH₄ shows a decrease tendency, changing from 87.5 to 18.3 µg/kJ with the increase in CO₂ proportion. The experimental results show that a higher CO₂/H₂ ratio is beneficial for CO selectivity. A higher H₂ ratio might contribute to further hydrogenation to produce methane, which is consistent with the observation in Fig. 4(b). According to Equations 19–21, the generation of CO needs less H₂ compared to methanol, as its stoichiometric ratio of CO₂/H₂ is only 1:1. To further explore the influence of the gas ratio on the selectivity of the products, we conduct the analysis from the electron-induced reactions and heavy species collisions-induced reactions. It can be found that plasma activates carbon dioxide and directly dissociates it into CO, while the generation of methane requires continuous hydrogenation reactions based on the CO intermediate. A higher hydrogen ratio is more conducive to the forward progress of the methane generation reaction, thereby increasing the selectivity of methane, which is consistent with our experimental results.

CO₂ is activated by the plasma and then dissociates into CO through Equation (22) or (23) (Mei et al., 2016). The CO₂ activation requires lower activation energies than the ground-level CO₂ molecule. Both excited and vibrational state CO₂ molecules have a much lower dissociation threshold (5.5 eV/molecule) than stable CO₂, which means plasma can accelerate the reduction of carbon dioxide into CO substantially (De et al., 2016).



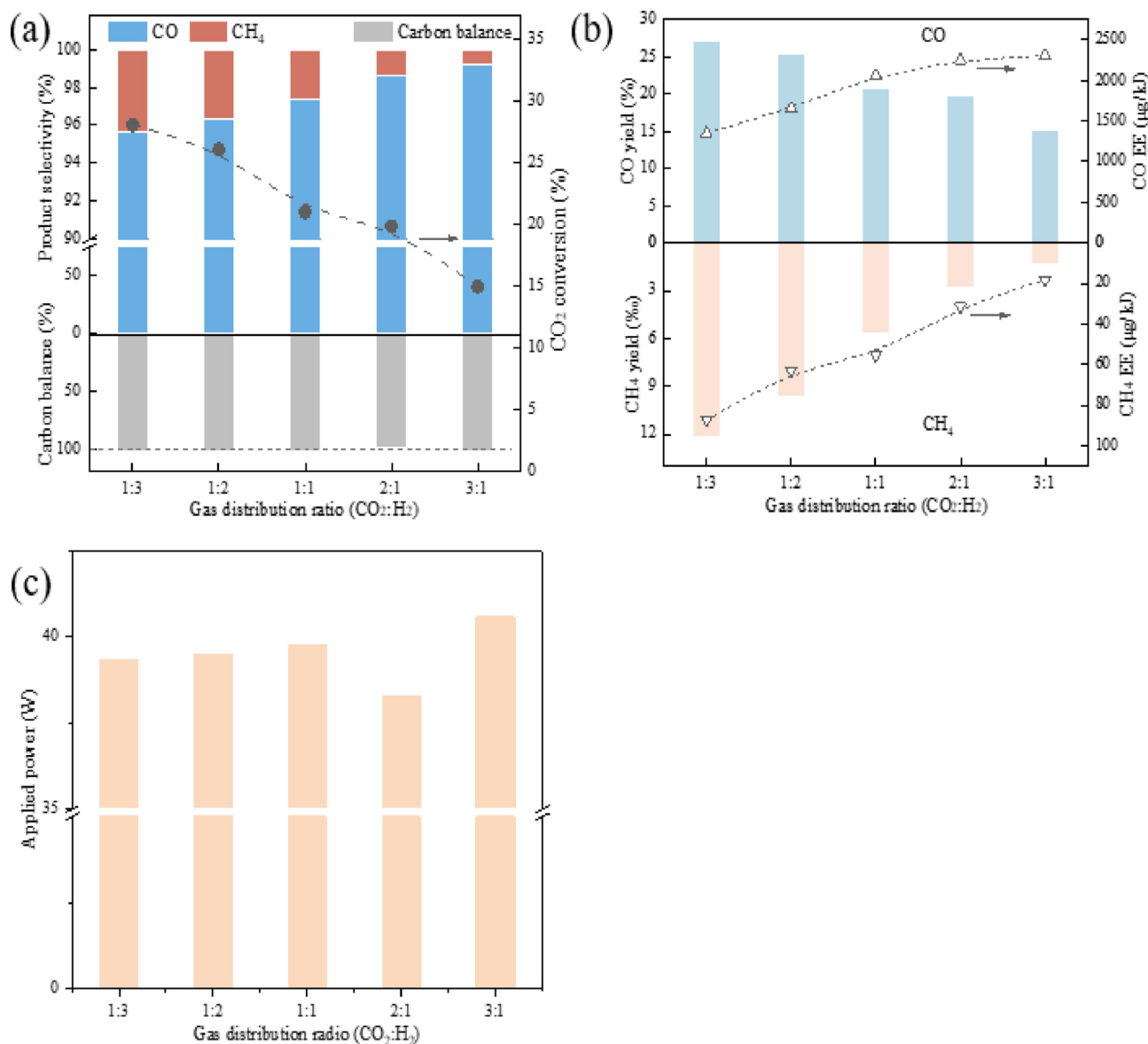


Fig. 4. The influence of CO₂/H₂ ratio on (a) CO₂ conversion, product selectivity, and carbon balance; (b) product yield and efficiency (CO and CH₄); (c) the applied power when the applied voltage is fixed at 4.5 kV (gas flow rate of 40 mL/min, applied power of 35 W, and discharge gap of 1 mm, respectively).

It is generally believed that plasma can generate high-energy electrons, which can collide with H₂ and CO₂ at high speed. It can not only activate CO₂ molecules to the excited state but also help facilitate the direct transformation of CO₂ and H₂ into CO and H radicals. Besides, hydrogen can also be dissociated in plasma because of its lower dissociation energy (4.4 eV). (Ahmad et al., 2020; De et al., 2016). The major reaction is the dissociation process through Equations 22–24, leading to a high CO selectivity of over 96% according to the experiments. Furthermore, radical recombination reactions between the O and H radicals lead to the generation of OH radicals, which are then recombined further into H₂O through Equation (26).



From the perspective of heavy species collision-induced reactions, the intermediate product CHO radicals are formed through the

recombination of H and carbon monoxide. Then methane is formed through further hydrogenation through Equations 27–30 (Zeng and Tu, 2017). The reaction path is as follows: CO₂→CO→CHO→CH₂O→CH₃O→CH₄. As a result, a lower CO₂/H₂ ratio is beneficial to the formation of methane, leading to a higher selectivity.



3.2.3. Influence of gas flow rate

The influence of gas flow rate is investigated in Fig. 5. Among all the products, CO still dominates as the main product with the selectivity above 90% regardless of the variation of gas flow rates. When the gas flow rate is set at 20 mL/min, the CO₂ conversion rate approaches its

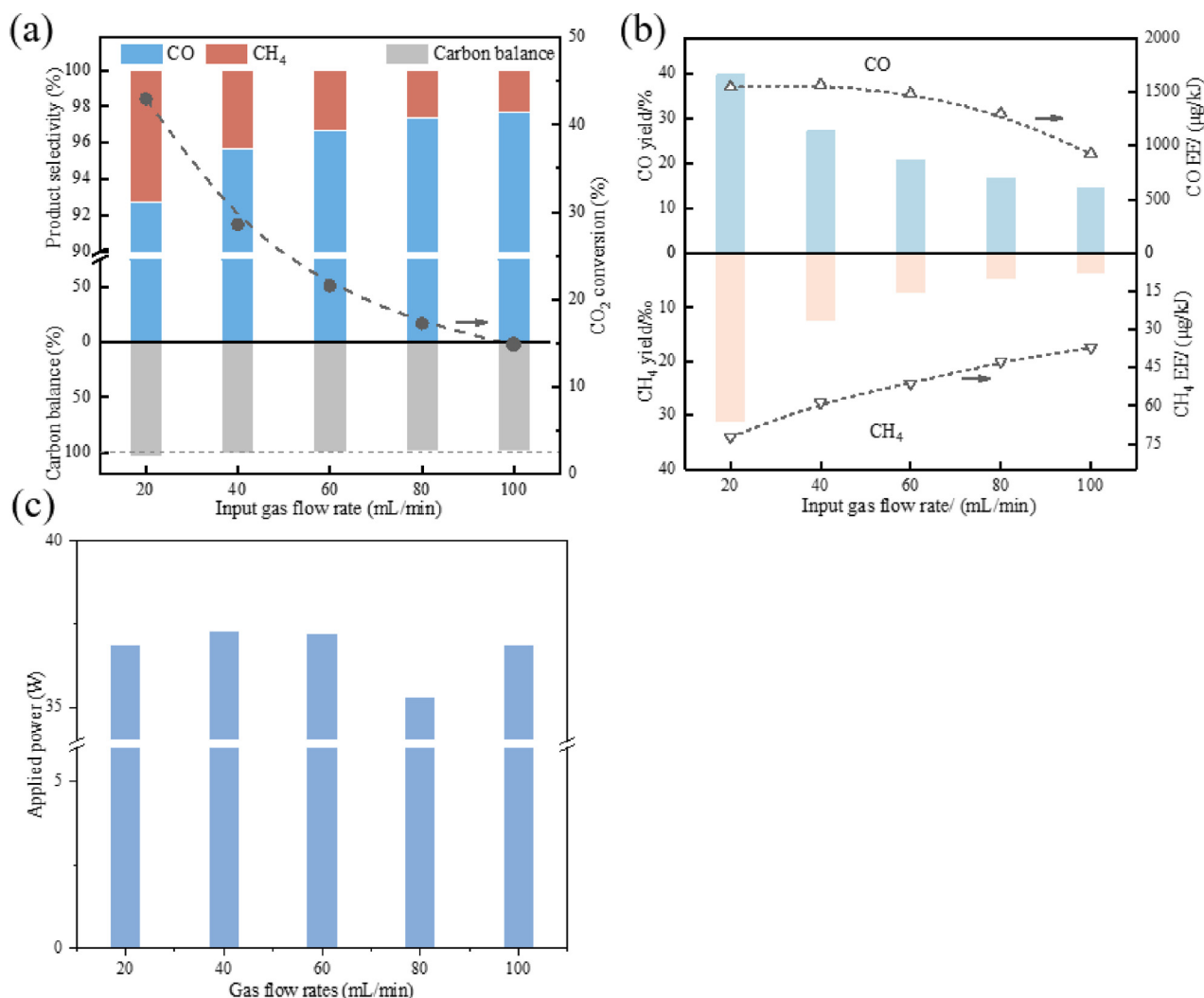


Fig. 5. The influence of gas flow rate on (a) CO₂ conversion, product selectivity, and carbon balance; (b) product yield and efficiency (CO and CH₄); (c) applied power (W) (CO₂/H₂ ratio of 1:3, applied power of 35W, and discharge gap of 1 mm).

maximum value of 43.0%, with a CO selectivity of 92.8%. With the gas flow rate increasing from 20 to 100 mL/min, the CO₂ conversion rate decreases from 43.0% to 14.8%. This is because a slower gas flow rate can extend the residence time, thereby increasing the possibility of collisions between reactants and active species or electrons in DBD plasma. On the other hand, from the perspective of thermodynamics, the RWGS reaction is a classical endothermic reaction according to Equations 19–21. Lower gas flow rates lead to a higher temperature at the reaction zone, which promotes the conversion of carbon dioxide to carbon monoxide. As a result, the energy efficiency of CO decreases from 1544.0 to 926.6 $\mu\text{g}/\text{kJ}$ with the increase of gas flow rate, while that of CH₄ increases from 37.0 to 72.3 $\mu\text{g}/\text{kJ}$.

Furthermore, the kinetic effects of flow rate on the reactions of CO and CH₄ are also different. Plasma activates carbon dioxide and directly dissociates it into CO, thereby initiating the rate-limiting step of methanation. The dissociation reaction steps of CO can be obtained according to Equations 22–24. Methane, on the other hand, needs to be continuously hydrogenated through multiple steps based on the CO intermediate according to Equations 27–30. The abundant supply of reactants generated by a higher flow rate may accelerate the reaction rate of CO generation because more carbon dioxide and hydrogen molecules participate in the reaction. However, the formation of CH₄ is a multi-step process with a relatively complex reaction mechanism and may not

respond as quickly as the CO generation to the increase in flow rate, resulting in a relatively slow increase in its reaction rate. Similarly, the CO generation reaction rate will decrease significantly due to the insufficiency of reactants when the flow rate decreases. Due to the characteristics of its multi-step process and continuous hydrogenation reduction, the decrease in the reaction rate is less significant compared to carbon monoxide. (Ullah et al., 2023).

In fact, the gas flow rate affects not only resident time and reaction temperature but also the specific energy density. Herein, the Pearson correlation coefficient is used to indicate the correlation between CO₂ conversion rate and specific energy density (SEI). From Table S1, a correlation coefficient value of 0.955 and a positive correlation level of 0.01 between the CO₂ conversion rate and SEI reveal a significant positive association between the CO₂ conversion rate and SEI. According to Fig. 6, a higher specific energy density can significantly enhance the conversion of CO₂ due to the increased energy input to the discharge. (Mei et al., 2016). Higher specific energy input generates more chemically reactive species, thereby significantly enhancing the electric field, electron density, and gas temperature within the discharge (Ozkan et al., 2017; Paulussen et al., 2010; Duan et al., 2015a, 2015b). All of them contribute variously to the carbon dioxide conversion and dissociation. A lower feed gas flow rate prolongs the retention time of the reactants, thereby further enhancing the conversion of reactants. (Mei et al., 2016).

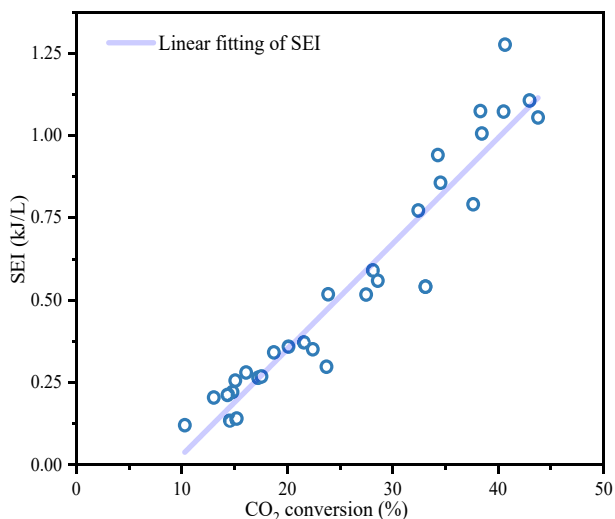


Fig. 6. The correlation relationship between specific energy density and CO₂ conversion rate.

3.2.4. The configuration of DBD plasma reactor

Apart from various operating conditions, the reactor configuration, including discharge gaps and types of ground electrode, also plays an important role in the performance of DBD plasma discharge. For instance, the discharge gap affects electric field density, which intimately relates to electron energy distribution and corresponding electron-induced reactions. Herein, the discharge gaps were tuned by changing the diameter size of the high-voltage electrode, and their influence on CO₂ hydrogeneation activation was investigated with the CO₂/H₂ ratio of 3:1 presented in Fig. 7. The CO₂ conversion rate reaches its optimum at a discharge gap of 2 mm. The extremely high electrode field strength at a small discharge gap leads to more collisions and dissociation between high-energy electrons and CO₂ molecules, eventually promoting the CO₂ conversion. However, if the discharge gap is too small (e.g., below 1 mm), the concentration of reaction products per unit volume is too high to affect the discharge stability. A discharge gap that is too wide will dilute the concentration of active species, thereby reducing the conversion of carbon dioxide. Besides, we also investigate the performance of the DBD reactor using different ground electrodes, as shown in Fig. 7(c). When the external stainless steel-made ground electrode is replaced by a circulating-water electrode, the CO₂ conversion rate decreases compared to the conventional metal electrode, especially at the lower applied

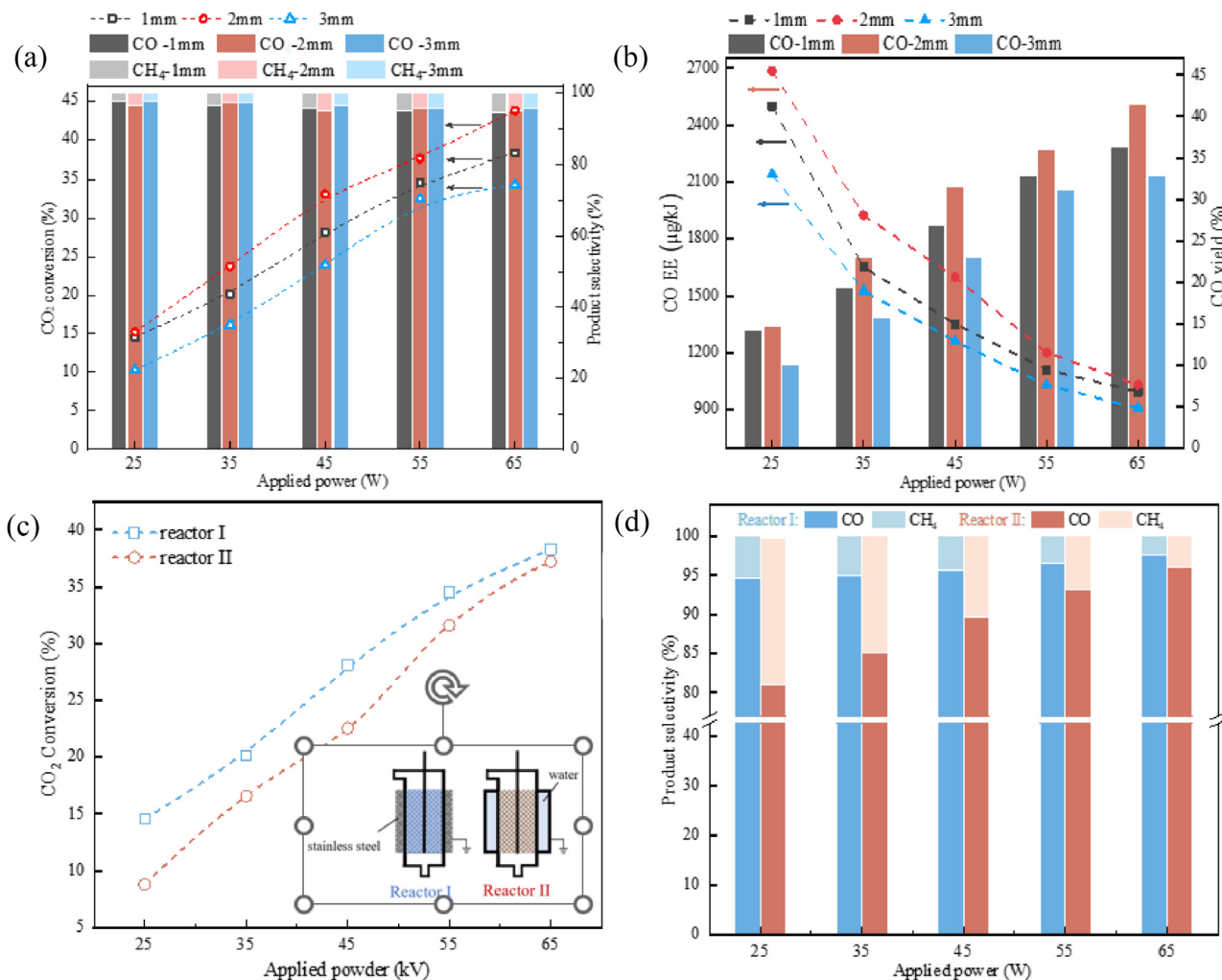


Fig. 7. The influence of discharge gaps on (a) CO₂ conversion and product selectivity; (b) product yield and energy efficiency of CO; Comparison of (c) CO₂ conversion and (d) product selectivity of metal-based electrode and water-based electrode in CO₂ hydrogeneation. (CO₂/H₂ ratio of 1:3 and applied power of 35W, respectively). The discharge gap is 1 mm.

voltage. The application of a circulating water-cooling jacket can switch the product from CO to CH₄ by reducing the temperature of the reaction zone, eventually improving the CH₄ selectivity prominently.

4. Conclusions

Single-variable experiments were designed to investigate the effects of operating conditions and reactor parameters. The carbon dioxide conversion and CO yield exhibit an upward trend with the increase of applied voltage due to the higher energy density distribution and more active species, reaching their maxima of 21.2% and 29.62%, respectively. On the contrary, the gas distribution ratio and flow rate have a distinct influence on the carbon dioxide hydrogenation. A higher H₂ ratio may contribute to the further hydrogenation to produce methane, while a slower gas flow rate can extend the residence time, thereby increasing the possibility of collisions between reactants, active species, and electrons. When the gas flow rate is set at 20 mL/min, the CO₂ conversion rate approaches its maximum value of 42.97% with a CO selectivity of 92.77%. Furthermore, we study the impact of reactor configuration by varying the discharge gaps and reactor types. The experimental results indicate that the CO₂ conversion rate reaches its optimum at a discharge gap of 2 mm, while a circulating water-cooling jacket can shift the product from CO to CH₄ by reducing the temperature of the reaction zone. The systematic consideration of DBD plasma-driven CO₂ hydrogenation is significant for further upgrading product value or integrating with other processes.

CRedit authorship contribution statement

Zhihao Zeng: Formal analysis, Investigation, Methodology, Writing – original draft. **Yujiao Li:** Data curation, Formal analysis, Investigation, Supervision, Writing – review & editing. **Yunfei Ma:** Investigation, Methodology. **Xiaoqing Lin:** Supervision. **Xiangbo Zou:** Methodology. **Hao Zhang:** Validation. **Xiaodong Li:** Supervision. **Qingyang Lin:** Supervision. **Ming-Liang Qu:** Investigation. **Angjian Wu:** Project administration, Resources, Supervision, Validation.

Declaration of competing interest

The authors declare that they have no known competing financial interests or personal relationships that could have appeared to influence the work reported in this paper.

Acknowledgements

This work is supported by the “Pioneer” and “Leading Goose” R&D Program of Zhejiang Province (2022C03016) and the Fundamental Research Funds for the Central Universities (2022ZJFH04).

Appendix A. Supplementary data

Supplementary data to this article can be found online at <https://doi.org/10.1016/j.gerr.2024.100102>.

References

- Aerts, R., Somers, W., Bogaerts, A., 2015. Carbon dioxide splitting in a dielectric barrier discharge plasma: a combined experimental and computational study[J/OL]. *ChemSusChem* 8 (4), 702–716. <https://doi.org/10.1002/cssc.201402818>.
- Ahmad, F., Lovell, E.C., Masood, H., et al., 2020. Low-temperature CO₂ methanation: synergistic effects in plasma-Ni hybrid catalytic system[J/OL]. *ACS Sustain. Chem. Eng.* 8 (4), 1888–1898. <https://doi.org/10.1021/acssuschemeng.9b06180>.
- Álvarez, A., Bansode, A., Urakawa, A., et al., 2017. Challenges in the greener production of formates/formic acid, methanol, and DME by heterogeneously catalyzed CO₂ hydrogenation processes[J/OL]. *Chem. Rev.* 117 (14), 9804–9838. <https://doi.org/10.1021/acs.chemrev.6b00816>.
- Brandenburg, R., Schiorlin, M., Schmidt, M., et al., 2023. Plane Parallel Barrier Discharges for Carbon Dioxide Splitting: influence of Discharge Arrangement on Carbon

- Monoxide Formation[J/OL]. *Plasma* 6 (1), 162–180. <https://doi.org/10.3390/plasma6010013>.
- Chaudhary, R., Van Rooij, G., Li, S., et al., 2020. Low-temperature, atmospheric pressure reverse water-gas shift reaction in dielectric barrier plasma discharge, with outlook to use in relevant industrial processes[J/OL]. *Chem. Eng. Sci.* 225, 115803. <https://doi.org/10.1016/j.ces.2020.115803>.
- Chen, H., Mu, Y., Xu, S., et al., 2020. Recent advances in non-thermal plasma (NTP) catalysis towards C1 chemistry[J/OL]. *Chin. J. Chem. Eng.* 28 (8), 2010–2021. <https://doi.org/10.1016/j.cjche.2020.05.027>.
- Chen, Q., Meng, S., Liu, R., et al., 2024. Plasma-catalytic CO₂ hydrogenation to methanol over CuO-MgO/Beta catalyst with high selectivity[J/OL]. *Appl. Catal. B Environ.* 342, 123422. <https://doi.org/10.1016/j.apcatb.2023.123422>.
- De, Bie C., Van, Dijk J., Bogaerts, A., 2016. CO₂ Hydrogenation in a Dielectric Barrier Discharge Plasma Revealed[J/OL]. *J. Phys. Chem. C* 120 (44), 25210–25224. <https://doi.org/10.1021/acs.jpcc.6b07639>.
- Duan, X., Hu, Z., Li, Y., et al., 2015a. Effect of dielectric packing materials on the decomposition of carbon dioxide using DBD microplasma reactor[J/OL]. *AIChE J.* 61 (3), 898–903. <https://doi.org/10.1002/aic.14682>.
- Duan, X., Li, Y., Ge, W., et al., 2015b. Degradation of CO₂ through dielectric barrier discharge microplasma[J/OL]. *Greenhouse Gases: Sci. Technol.* 5 (2), 131–140. <https://doi.org/10.1002/ggh.1425>.
- Eliasson, B., Kogelschatz, U., Xue, B., et al., 1998. Hydrogenation of Carbon Dioxide to Methanol with a Discharge-Activated Catalyst[J/OL]. *Ind. Eng. Chem. Res.* 37 (8), 3350–3357. <https://doi.org/10.1021/ie9709401>.
- George, A., Shen, B., Craven, M., et al., 2021. A Review of Non-Thermal Plasma Technology: A novel solution for CO₂ conversion and utilization[J/OL]. *Renew. Sustain. Energy Rev.* 135, 109702. <https://doi.org/10.1016/j.rser.2020.109702>.
- Huang, W., Yue, W., Dong, Y., et al., 2023. Field parameters investigation of CO₂ splitting in atmospheric DBD plasma by multi-physics coupling simulation and emission spectroscopy measurements[J/OL]. *Fuel* 353, 129236. <https://doi.org/10.1016/j.fuel.2023.129236>.
- IEA, 2020. CCUS in Clean Energy transitions[R]. IEA, Paris.
- Kanuri, S., Dinda, S., Singh, S.A., et al., 2024. Microrod networks CuO–ZnO–Al₂O₃ catalyst for methanol synthesis from CO₂: Synthesis, characterization, and performance demonstration[J/OL]. *Mater. Today Chem.* 36, 101959. <https://doi.org/10.1016/j.mtchem.2024.101959>.
- Karakaya, C., Parks, J., 2023. Thermochemical processes for CO₂ hydrogenation to fuels and chemicals: Challenges and opportunities[J/OL]. *Applications in Energy and Combustion Science* 15, 100171. <https://doi.org/10.1016/j.jaecs.2023.100171>.
- Kondratenko, E.V., Mul, G., Baltrusaitis, J., et al., 2013. Status and perspectives of CO₂ conversion into fuels and chemicals by catalytic, photocatalytic and electrocatalytic processes[J/OL]. *Energy Environ. Sci.* 6 (11), 3112. <https://doi.org/10.1039/c3ee41272e>.
- Li, Y., Yu, H., Dai, J., et al., 2023. CH₄ and CO₂ conversion over boron nitride-supported Ni catalysts with BO defects in DBD plasma[J/OL]. *Fuel Process. Technol.* 242, 107655. <https://doi.org/10.1016/j.fuproc.2023.107655>.
- Mahdikia, H., Brüser, V., Schiorlin, M., et al., 2023. CO₂ Dissociation in Barrier Corona Discharges: Effect of Elevated Pressures in CO₂/Ar Mixtures[J/OL]. *Plasma Chem. Plasma Process.* 43 (6), 2035–2063. <https://doi.org/10.1007/s11090-023-10411-1>.
- Mei, D., Zhu, X., Wu, C., et al., 2016. Plasma-photocatalytic conversion of CO₂ at low temperatures: Understanding the synergistic effect of plasma-catalysis[J/OL]. *Appl. Catal. B Environ.* 182, 525–532. <https://doi.org/10.1016/j.apcatb.2015.09.052>.
- Modak, A., Bhanja, P., Dutta, S., et al., 2020. Catalytic reduction of CO₂ into fuels and fine chemicals[J/OL]. *Green Chem.* 22 (13), 4002–4033. <https://doi.org/10.1039/D0GC01092H>.
- Olah, G.A., Goepfert, A., Prakash, G.K.S., 2009. Chemical Recycling of Carbon Dioxide to Methanol and Dimethyl Ether: From Greenhouse Gas to Renewable, Environmentally Carbon Neutral Fuels and Synthetic Hydrocarbons[J/OL]. *J. Org. Chem.* 74 (2), 487–498. <https://doi.org/10.1021/jo801260f>.
- Ozkan, A., Bogaerts, A., Reniers, F., 2017. Routes to increase the conversion and the energy efficiency in the splitting of CO₂ by a dielectric barrier discharge[J/OL]. *J. Phys. Appl. Phys.* 50 (8), 084004. <https://doi.org/10.1088/1361-6463/aa562c>.
- Paulussen, S., Verheyde, B., Tu, X., et al., 2010. Conversion of carbon dioxide to value-added chemicals in atmospheric pressure dielectric barrier discharges[J/OL]. *Plasma Sources Sci. Technol.* 19 (3), 034015. <https://doi.org/10.1088/0963-0252/19/3/034015>.
- Peeters, F.J., Van de Sanden, M.C., 2014 Dec 9. The influence of partial surface discharging on the electrical characterization of DBDs. *Plasma Sources Sci. Technol.* 24 (1), 015016.
- Ray, D., Chawdhury, P., Bhargavi, K.V.S.S., et al., 2021. Ni and Cu oxide supported γ -Al₂O₃ packed DBD plasma reactor for CO₂ activation[J/OL]. *J. CO₂ Util.* 44, 101400. <https://doi.org/10.1016/j.jcou.2020.101400>.
- Schwiderowski, P., Ruland, H., Muhler, M., 2022. Current developments in CO₂ hydrogenation towards methanol: A review related to industrial application[J/OL]. *Curr. Opin. Green Sustainable Chem.* 38, 100688. <https://doi.org/10.1016/j.cogsc.2022.100688>.
- Shin, H., Hansen, K.U., Jiao, F., 2021. Techno-economic assessment of low-temperature carbon dioxide electrolysis[J/OL]. *Nat. Sustain.* 4 (10), 911–919. <https://doi.org/10.1038/s41893-021-00739-x>.
- Tada, S., Kinoshita, H., Ochiai, N., et al., 2021. Search for solid acid catalysts aiming at the development of bifunctional tandem catalysts for the one-pass synthesis of lower olefins via CO₂ hydrogenation[J/OL]. *Int. J. Hydrogen Energy* 46 (74), 36721–36730. <https://doi.org/10.1016/j.ijhydene.2021.09.002>.
- Ullah, N., Su, M., Yang, Y., et al., 2023. Enhanced CO₂ hydrogenation to light hydrocarbons on Ni-based catalyst by DBD plasma[J/OL]. *Int. J. Hydrogen Energy* 48 (57), 21735–21751. <https://doi.org/10.1016/j.ijhydene.2023.03.006>.

- Wanten, B., Vertongen, R., Meyer, R.D., et al., 2023. Plasma-based CO₂ conversion: How to correctly analyze the performance?[J/OL]. *J. Energy Chem.* 86 (11), 180. <https://doi.org/10.1016/j.jechem.2023.07.005>.
- Wei, Y.M., Kang, J.N., Liu, L.C., et al., 2021. A proposed global layout of carbon capture and storage in line with a 2°C climate target[J/OL]. *Nat. Clim. Change* 11 (2), 112–118. <https://doi.org/10.1038/s41558-020-00960-0>.
- Wu, H., Xiong, S., Liu, C jun, 2023. Preparation of In₂O₃/ZrO₂ catalyst via DBD plasma decomposition of Zr(OH)₄ for CO₂ hydrogenation to methanol[J/OL]. *Catal. Today* 423, 114024. <https://doi.org/10.1016/j.cattod.2023.02.001>.
- Zeng, Y., Tu, X., 2017. Plasma-catalytic hydrogenation of CO₂ for the cogeneration of CO and CH₄ in a dielectric barrier discharge reactor: effect of argon addition[J/OL]. *J. Phys. Appl. Phys.* 50 (18), 184004. <https://doi.org/10.1088/1361-6463/aa64bb>.
- Zhai, M., Huang, G., Liu, H., et al., 2020. Three-perspective energy-carbon nexus analysis for developing China's policies of CO₂-emission mitigation[J/OL]. *Sci. Total Environ.* 705, 135857. <https://doi.org/10.1016/j.scitotenv.2019.135857>.
- Zhang, Y., Wang, B., Ji, Z., et al., 2023. Plasma-catalytic CO₂ methanation over NiFe/(Mg, Al)₂O₃ catalysts: Catalyst development and process optimisation[J/OL]. *Chem. Eng. J.* 465, 142855. <https://doi.org/10.1016/j.cej.2023.142855>.